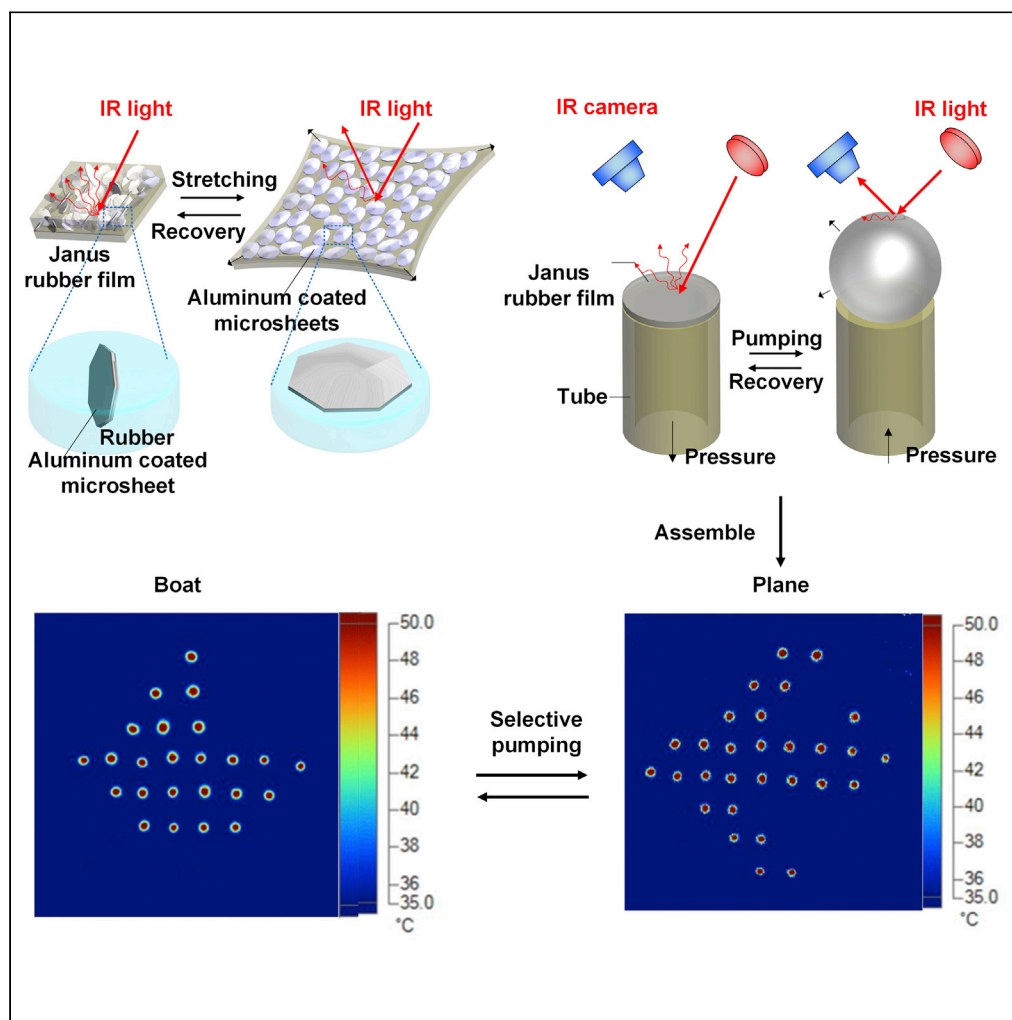**Article**

Facile, scalable, and adaptive infrared reflection towards soft systems by blowing a Janus rubber film

Linghui Peng, Jianyu Huang, Ruiping Zou, Bin Su

subin@hust.edu.cn

Highlights

The IR reflection can be tuned by the expansion/ recovery of the Janus rubber film.

A pixilated device can adaptively IR camouflage/ display through selected blowing.

The assembled tube arrays exhibit fast response and can be scalable manufactured.

Article

Facile, scalable, and adaptive infrared reflection towards soft systems by blowing a Janus rubber film

Linghui Peng,[1,2] Jianyu Huang,[1] Ruiping Zou,[2] and Bin Su[1,3,*]

SUMMARY

Controllable IR-reflection systems can be applied to displays, adaptive military camouflages, thermal managements, and many other fields. However, current reported controllable IR-reflection systems suffer from utilizing rigid materials, complicated devices, or high working temperature/voltage, which are not suitable for their widespread applications toward soft systems. Herein, inspired by cephalopods, we demonstrate a facile and scalable method for adaptive IR reflection based on a Janus rubber film, which is composed of aluminum-coated microsheets (AMSs)/rubber composite top and a rubber only bottom. Expansion of the Janus rubber film causes random arrangement of AMSs to stay planar, resulting in the change from IR scattering to concentrated IR reflection. By fixing the Janus rubber films upon the arranged tubes, as-prepared arrays could display complex and changeable patterns by selectively pumping tubes. Being facile and of general validity, our strategies broaden the scope of future controllable IR reflecting applications for environmental IR camouflages and displays.

INTRODUCTION

A continuous-range tuning of infrared (IR) features upon matters can enable innovative technologies and applications, such as building insulations (Granqvist et al., 2017; Hu et al., 2018), energy-conserving windows (Ke et al., 2018; Lee et al., 2019; Liu et al., 2016), protective clothing (Cai et al., 2017; Jiang et al., 2016; Peng et al., 2020), and adaptive IR camouflages for military and commercial purposes (Yu et al., 2014; Chandrasekhar et al., 2003; Zhu et al., 2020; Gu et al., 2020). Two main mechanisms are now established, including the modulation of IR emittance and the control of IR reflection (Li et al., 2020a). The former mechanism usually utilizes microfluidics-based or thermoelectric systems by injecting hot/cool liquids or special thermoelectric materials, respectively (Morin et al., 2014; Hong et al., 2020). However, they suffer from slow response time, complex preparation processes, and changing of their real temperatures. The latter one bases on metals, metal oxides, graphenes, conductive polymers, and metastructures to modulate the IR reflection without changing their own temperatures (Li et al., 2020b; Mandal et al., 2018; Chandrasekhar et al., 2002). Commonly, their working mechanisms are divided into three types, including thermochromic, electrochromic, and mechanochromic devices.

IR thermochromic materials (Dai et al., 2013; Ji et al., 2018), such as VO_2 and its composites, can exhibit considerable IR reflection changes because of their thermally induced phase transitions yet limited by fixed working temperature (Xu et al., 2018a). IR electrochromic devices (Xu et al., 2018b, 2020; Leung et al., 2019) are able to tune the IR reflection by electrochemical redox reactions or metal electrodeposition but struggle with the comparatively low IR emittance tunabilities and narrow IR modulation ranges. Mechanochromic devices combining metal thin films and elastic polymers can rapidly modulate their IR reflections by forming cracks or wrinkles under mechanical force; however, they are restricted by narrow IR modulation ranges and hysteresis during cycling (Tian et al., 2017; Chandrasekhar et al., 2002; Salihoglu et al., 2018). Notably, above-mentioned approaches are not scalable manufactured, high temperature/voltage dependent, and commonly rigid, which might not be suitable for practical applications. Thus, a facile (simple materials and setup) and easy-to-scale-up method to engineer the adaptive IR reflection for soft systems (such as soft robots) is urgently needed.

Learning from nature is a powerful resource to design new material systems (Golnaz and Marco, 2018; Wang et al., 2014). Cephalopods are the king of adaptive camouflage in visible and IR range (Mathger et al., 2009; Mathger and Hanlon, 2007; Yang et al., 2021). Their skin surfaces contain numerous

[1]State Key Laboratory of Material Processing and Die & Mould Technology, School of Materials Science and Engineering, Huazhong University of Science and Technology, Wuhan 430074, Hubei, P. R. China

[2]ARC Hub for Computational Particle Technology, Department of Chemical Engineering, Monash University, Clayton VIC 3800, Australia

[3]Lead contact

*Correspondence:
subin@hust.edu.cn

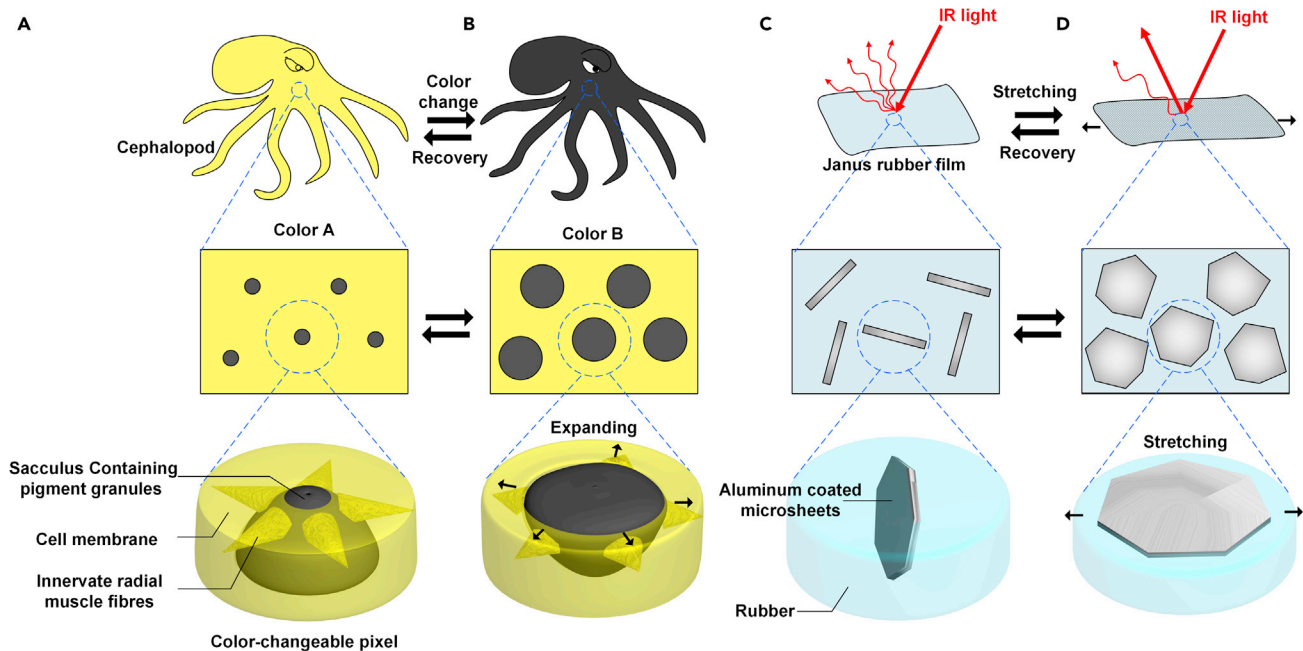https://doi.org/10.1016/j.isci.2021.102430

Figure 1. Working mechanism of chromatophore cells

(A and B) The cephalopod in yellow color changes to black color, and the appearances of color-changing skins before and after being triggered by external stimuli, respectively. Schematic diagrams of one chromatophore cell consisting of pigment-loading sacculus and surrounding radial muscles before and after being triggered by external stimuli.

(C and D) The Janus rubber film scatters and reflects IR light before and after stretching, respectively. Schematic diagrams of one aluminum-coated microsheet (AMS) and surrounding rubber acting as a chromatophore cell before and after being triggered by external stimuli. The AMSs in Janus rubber film arranges randomly at pristine stage and arranges planar after stretching.

chromatophores and structural reflectors, which can tune the interaction between the light and the skins through the muscle contraction and expansion (Phan et al., 2016). Inspired by cephalopods, herein we demonstrate a facile and scalable method for adaptive IR reflection based on a Janus rubber film, which is composed of an AMS/rubber composite top and a rubber-only bottom. The apparent IR reflection was dramatically changed following the expansion/recovery of the Janus rubber film. In addition, such Janus rubber films were easy to construct a pixilated device that can control IR reflection of each pixel upon selected actuation, exhibiting changeable IR patterns for environmental camouflages and displays. Our adaptive-IR-reflection system simultaneously possesses simple actuation mechanism, room working temperature, controllable response (depends on pumping system), stability to repeated cycling (100 cycles), amenability to patterning and multiplexing, and straightforward manufacturability.

RESULTS

Structure of the Janus rubber film

Generally, quick change of cephalopods' skin colors relies on the chromatophore cells, which consist of the pigment-loading sacculus and surrounding radial muscles (Figure 1). Cell membranes (color A) cover most area of the sacculus (color B), thus appearing (color A) as shown in Figure 1A. Being triggered by the nerve signals, radial muscles would contract, yielding the planar expansion of the sacculus, as well as the color change of the whole appearance of skin (color B) as shown in Figure 1B. Inspired by cephalopods, we prepared a Janus rubber film that consists of aluminum-coated microsheets (AMSs)/rubber top and a rubber-only bottom. The AMSs in the film are randomly arranged at pristine status, yielding IR scattering (Figure 1C). In contrast, being actuated by the external force, the stretched film led to the planar arrangement of AMSs, yielding the change from the diffuse IR scattering to the concentrated IR reflection (Figure 1D).

The fabrication process of the Janus film was as follows. A flat plate coated with a thin calcium nitrate layer was submerged in the rubber solution to coat the first rubber-only layer (Figure 2A). Then, the plate underwent the second submersion in an AMSs/rubber mixture solution (AMSs were shown in Figure S1), resulting
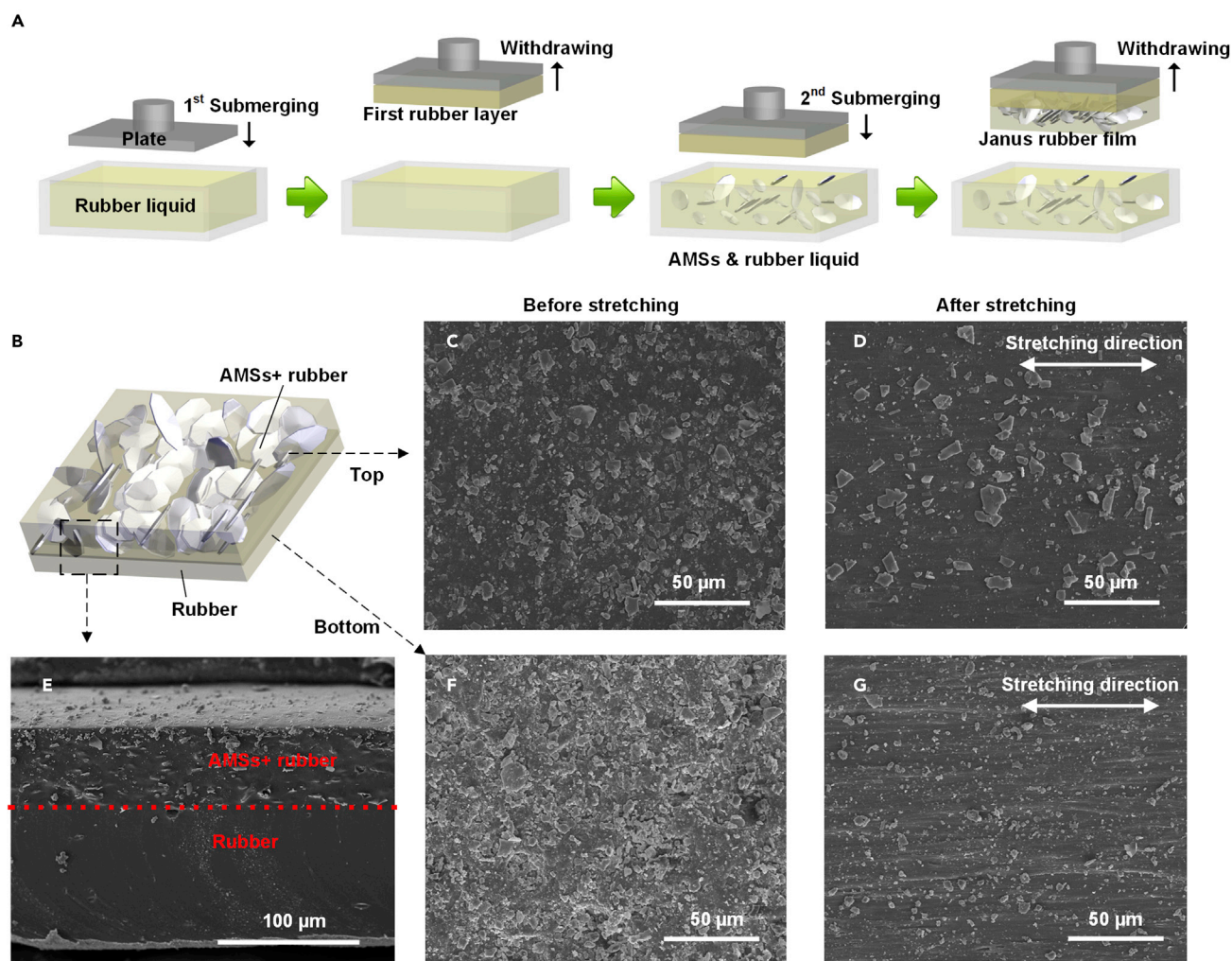
Figure 2. A Janus rubber film

(A) Preparation procedure of the Janus rubber film.

(B) Schematic diagram of structure of the Janus rubber film.

(C and D) SEM images of top surface of the Janus rubber film before and after stretching, respectively.

(E) SEM image of cross-section of the Janus rubber film.

(F) and (G) SEM images of bottom surface of the Janus rubber film before and after stretching, respectively.

in a Janus rubber film after drying in oven at 80°C (Figure 2B). Figure 2C shows the top view SEM image of the Janus rubber film. The AMSs on the top layer were randomly arranged before stretching, indicating a rough surface to multi-directionally scatter IR light. In contrast, those AMSs were planarly arranged when the film was horizontally stretched (Figure 2D). Optical microscopy images in Figure S2 also reveal that more planar AMSs appeared and surface roughness decreased when the film was uniaxially stretched. On the other side, the bottom of the Janus rubber film was mostly filled with rubber granules no matter before (Figure 2F) or after (Figure 2G) uniaxial stretching. From the cross-sectional SEM image in Figure 2E, the thickness of as-prepared Janus rubber film was around 220 μm.

The Janus rubber film showed controllable IR reflection capacity through the mechanical stretching. The digital images of a Janus rubber film with uniaxial stretching strain ranging from 0%, 30%, 60%, 80%, and 100% are presented in Figures 3A–3E, respectively, which shows gray color due to AMSs. Correspondingly, the IR images (Figures 3F–3J) indicate that the apparent surface temperatures of the Janus rubber film increased significantly from 31.5°C to 60.1°C (~28.6°C increase) with the rise of stretching strain under IR radiation for 1 min. The planar arrangement of AMSs increased with the rise of the stretching strain,
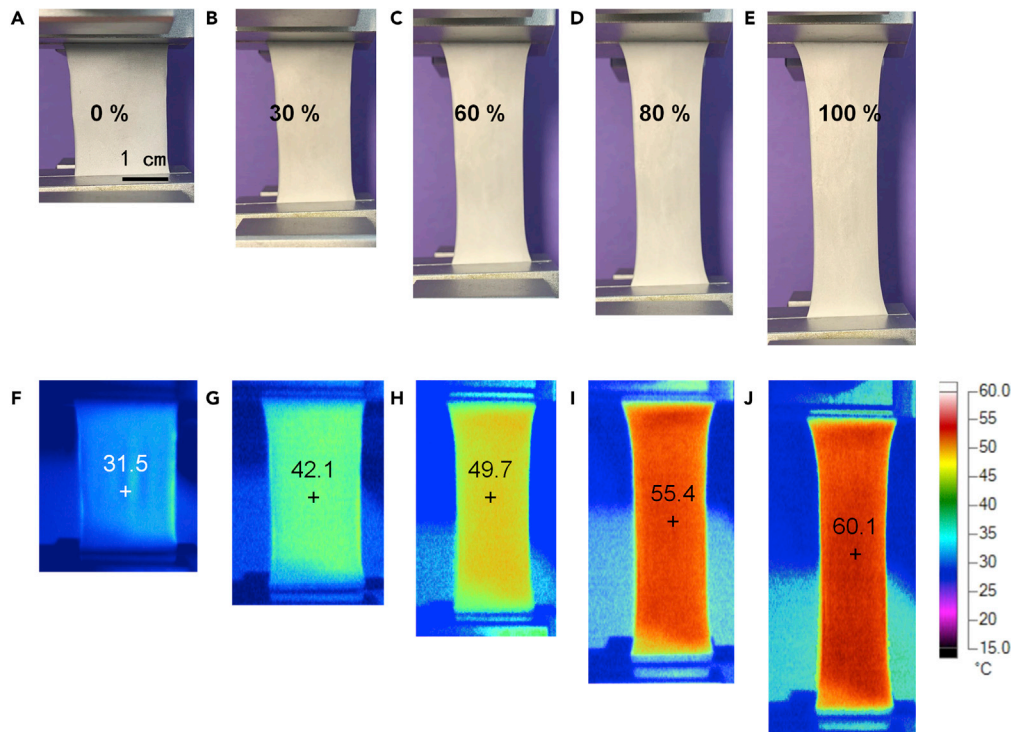
Figure 3. Controllable IR reflecting and camouflage of the Janus rubber film
(A–E) Digital images of the Janus rubber film with stretching strain of 0%, 30%, 60%, 80%, and 100%, respectively.
(F–J) Their corresponding IR images under IR radiation for 1 min.

resulting in more IR light reflection toward IR camera. Actually, the apparent surface temperatures of the Janus rubber film are closed before and after stretching without IR radiation (Figure S3). These results indicate that the IR reflection of the Janus rubber film could be controllably tailored through a mechanical stretching.

Working mechanism

The working mechanism of our controllable IR reflecting strategy is similar to that of cephalopods' chromatophore cells (Figure 1). The rubber part served as the expansible radial muscles, whereas the AMSs played a role as the sacculus. Before stretching, the randomly arranged AMSs on the top of the film would scatter the IR light (Figure 4A), leading to a low surface temperature observed by IR camera. In contrast, the AMSs were planar arranged with the expansion of rubber film (Figures 2 and S2), reflecting the IR light to a certain angle to be observed by IR camera. Thus, the observed surface temperature of the stretched Janus rubber film would be higher than that of the unstretched one. Different from other works inspired by cephalopods, which wrinkle (Xu et al., 2018b) or crack the metallic (Leung et al., 2019) or polymer thin films (Xu et al., 2020) on the elastic polymer film for tuning IR reflection, our design bases on the arrangements of the separated metallic microsheets embedded in rubber matrix to control the diffusion or concentrated reflection of IR lights. The separated metallic microsheets could be protected by rubber matrix, yielding stability for cycling and facile preparation.

We investigated the IR modulating capability of the Janus rubber film by testing its IR reflection with a biaxial stretching strain ranging from 0% to 100% (Figure 4B). Owing to the IR reflection of AMSs, the reflection gradually increased from 40% to 80% (Figure 4C) with the increase of stretching strain (the reflection centered at 1000 nm was used for this quantitative analysis). As shown in Figure 4C, the reflection of IR light at 1000 nm increases significantly when the Janus rubber film was stretched. Based on these spectra results, it can be summarized that the stretching led to rearrangement of AMSs in the rubber film, allowing to the reflection of IR light toward a focused direction. Thus, a sharp increase of the surface temperature appeared on the stretched Janus rubber film.
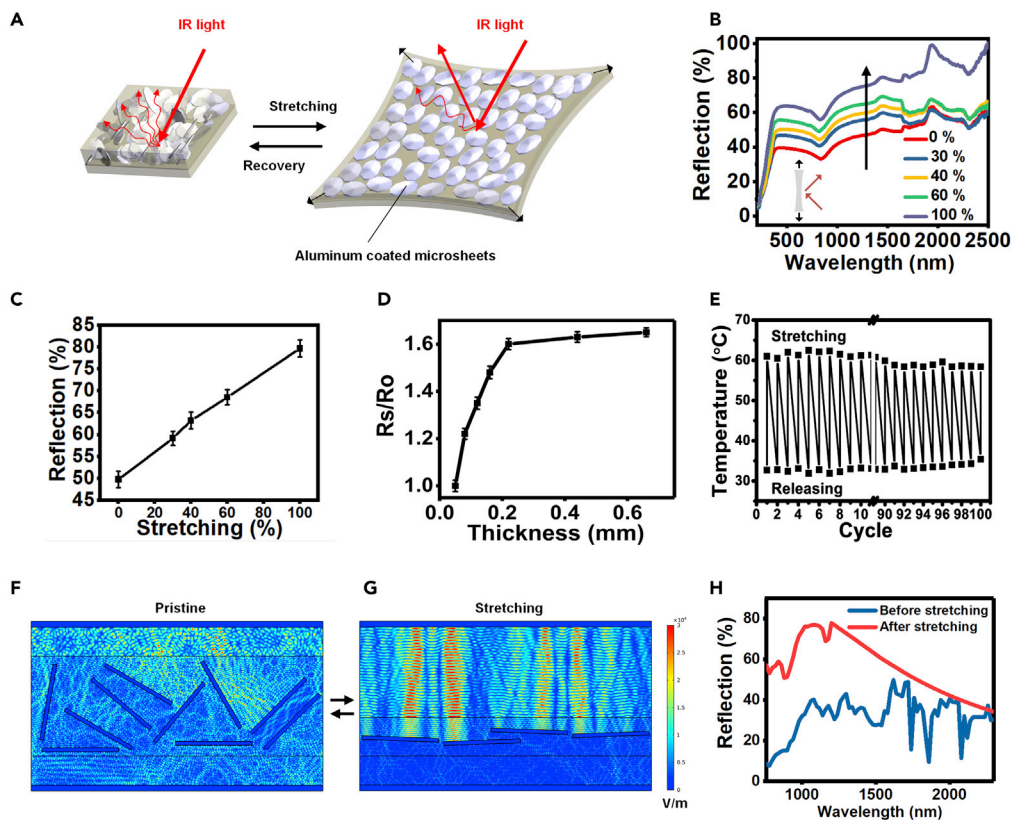
Figure 4. Working mechanism of the Janus rubber film to tune IR reflection

(A) Schematic diagram of the IR reflection change upon the Janus rubber film in pristine and stretched states. In pristine status, AMSs were randomly dispersed in the rubber film, resulting in a rough surface to scatter the IR light toward different directions. In contrast, the expanding of the rubber film results in planar arrangement of AMSs along the stretched surface. In this case, the IR light can be directionally reflected toward the IR camera, leading to the sharp apparent temperature increase.

(B) Reflection spectra of the Janus rubber film with a biaxial stretching strain ranging from 0% to 100%.

(C) Reflection centered at 1000 nm according to (B). Data were represented as mean $\pm$ sem (n = 5).

(D) The dependence of reflection ratio after and before 100% stretching on the rubber thicknesses. Data were represented as mean $\pm$ sem (n = 5).

(E) Representative 100 cycles of alternative surface temperatures of the Janus rubber film before and after expanding.

(F and G) Electromagnetic wave simulations on the Janus rubber film before and after stretching, respectively.

(H) Simulated IR reflection curves of the Janus rubber film before and after stretching.

We investigated the dependence of the reflection ratio after/before 100% stretching on the film thickness (Figure 4D). Lager ratio indicates a better IR reflection tuning ability of the film. The maximum ratio occurs at a thickness value of 0.2 mm, whereas it does not further increase with increase of thickness. Thus, the thickness of rubber films in further experiments was fixed at 0.2 mm. To investigate cycling duration of the Janus rubber film, we used IR camera to test the apparent surface temperature of the Janus rubber film after/before stretching under IR radiation for representative 100 cycles (Figure 4E). The apparent surface temperature on the Janus rubber film stably switched between 22°C and 55°C during stretching cycles. No significant temperature decreases after 100 cycles.

Besides spectra observations, the qualitative electromagnetic wave simulations upon the top 25 μm layer of Janus rubber film under IR radiation before and after stretching with 100% strain were conducted, investigating the influence of AMSs rearrangement on the IR reflections. As shown in Figure 4F, dark blue lines represent the cross sections of the several AMSs in the top Janus rubber film. The color contrast shows the density of IR light. In the pristine state, IR light could be scattered by the AMSs with random arrangement, leading to dispersive IR light in all directions, and a few IR light could even go through the AMSs. On the
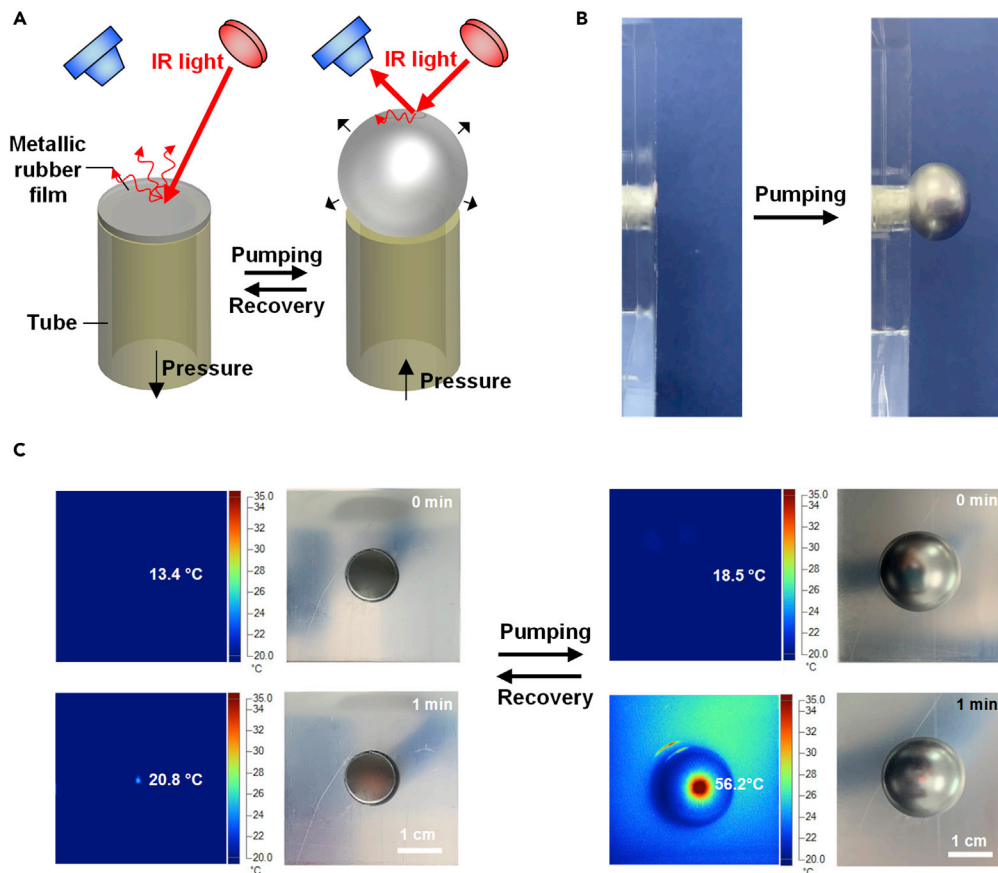
Figure 5. Facile and rapid IR reflection change by the blowing strategy
(A) Schematic diagram of blowing-assisted IR reflection change. A tube was covered by a Janus rubber film. When being blown, the apparent surface temperature of the tube top was changed sharply.
(B) Digital photos of cross sections of the tube top before and after blowing.
(C) Digital photos (right) and corresponding IR images (left) of the blowing-assisted IR reflection change before (top) and after (bottom) being radiated for 1 min.

contrast, IR light was mostly reflected back to the incident direction when the Janus film was horizontally stretched, in which the AMSs were planarly arranged toward the same direction (Figure 4G). The red color on the top of the AMSs indicates high intensity of IR light, whereas dark blue on the bottom of the AMSs means that very less IR light would go through the AMSs. Accordingly, the simulated IR reflections of the Janus rubber film before/after stretching were calculated, as shown in Figure 4H. A significant reflection increase in vertical direction can be observed after stretching, which is in accordance with the experimental results (Figure 4B).

For control experiments, we fabricated a single-layer rubber-only film, as well as a single-layer AMS/rubber composite film, and investigated their capacities for IR modulation (Figure S4). Unfortunately, the rubber-only film was too transparent to reflect IR light no matter in the pristine or stretched states. On the other hand, the AMSs/rubber composite layer struggled with the leaking problem. Cracks were obvious under the stretching, which would result in defects of IR reflection. Therefore, the Janus rubber film shows better performance to modulate IR radiation, whose top AMSs/rubber layer realized tunable IR reflection, whereas the bottom rubber-only layer ensured the robust mechanical substrate for stretching.

Facile and rapid control of IR reflection by blowing the Janus rubber film

We demonstrate a prototype blowing-assisted IR reflecting model in Figure 5A. A plastic or metallic tube, with an internal diameter of ~1 cm, was firmly covered and sealed by a Janus rubber film (more details can

be found in transparent method). The bottom of the tube was connected with a propulsion setup to provide a controlled pumping force (pneumatic bulging was chosen as a representative pumping strategy as shown in Figure S5). Before actuation, the Janus rubber film on the tube top was flat (Figure 5B left). When pumping the tube, and then maintaining a certain static pressure, the Janus rubber film would be greatly expanded (Figure 5B right). Notably, the surface of the tube top was blown to a semispherical shape and suddenly changed its IR reflection detected by the IR camera (Figure S6).

Before IR radiation, the apparent surface temperature of the flat Janus rubber surface was around 13°C (Figure 5C left top). Even if it was expanded to hemisphere, the surface temperature only increased to 18.5°C due to IR radiation from the background environment. Notably, being radiated by a 1200 W IR source for 1 min, the temperature of the flat surface just rose to 20.8°C while that of the blown counterpart sharply increased to 56.2°C, indicating a ∼6 times increase of temperature change by the blowing strategy. It was obvious that a highlight spot existed on the blown surface, which concentratively reflected IR light. When being blown, IR light could be directionally reflected toward to the IR camera, leading to the sharp temperature increase spot. This supposition was also confirmed by directly stretching the Janus rubber films (Figure 3).

Changeable IR display and camouflage

Owing to blowing-assisted IR reflection changes of the Janus rubber surface, such a simple method can be applied to IR display and camouflage (Figure 6). We assembled 4 × 4 arrays, in which each tube was independently controlled to serve as an IR pixel, allowing the color contrast under IR radiation through the IR camera observation. We selectively pumped the certain tubes (Figure 6A), showing the IR patterns of "C," "H," "I," "N," and "A" (Figure 6B). Each blown pixel featured an increased apparent temperature difference of ∼8°C between the focusing spot on the Janus rubber surface and the background, including the surrounding flat rubber films and the environment.

Finally, we demonstrate the ability of our blowing-assisted arrays for camouflage (Figure 6C). Similar to above setup, we assembled 9 × 8 arrays with smaller diameters (more tubes can be assembled if needed). At the beginning, we selectively pumped the certain tubes to form a car shape under IR radiation. From the IR camera observation (Figure 6D left), a car shape pattern can be found, whose spots have ∼13°C higher apparent temperature than the surroundings. Then, we changed the pumped tubes, allowing the IR patterns to be a plane (Figure 6D middle) or a boat (Figure 6D right). Theoretically, we can display on-demand IR patterns by designing the pumping parameters of the tubes. The change of IR patterns by this blowing-assisted method is rapid (within seconds depending on the pumping setup), stable, scalable, and programmable. Thus, it might find promising application for the IR camouflage and display after upgrading their pixel densities and/or sizes.

DISCUSSION

We have designed a Janus rubber film to control IR reflection and conceptualized and validated a new strategy for a facile, rapid, and on-demand IR reflecting device through blowing the Janus rubber film. Several advantages can be found in this approach. First and the most important one, our method utilizes low-cost and even commercial products, rather than special synthetic materials, to realize adaptive IR reflection. Second, the arrangement of the tubes can serve as pixel arrays to display complex patterns by selective pumping of desired tubes. Future development of this study focuses on the optimization of the propulsion setup for minimization. This blowing-assisted strategy involving adaptive IR reflection shows great potential for displays and camouflages in the civil and military applications.

Limitations of study

The limitations of our study are relatively low resolution of the assembled devices and the immature pumping system. First, in this study, the diameter of the assembled tubes is relatively large for high resolution of IR camouflage and display. A smaller diameter of the tube would be necessary for a high-resolution IR reflection. Second, our pneumatic pumping system is not programmable and automatic controlled. For better and quicker IR camouflage and display, a more sophisticated pumping and releasing control system would be designed.
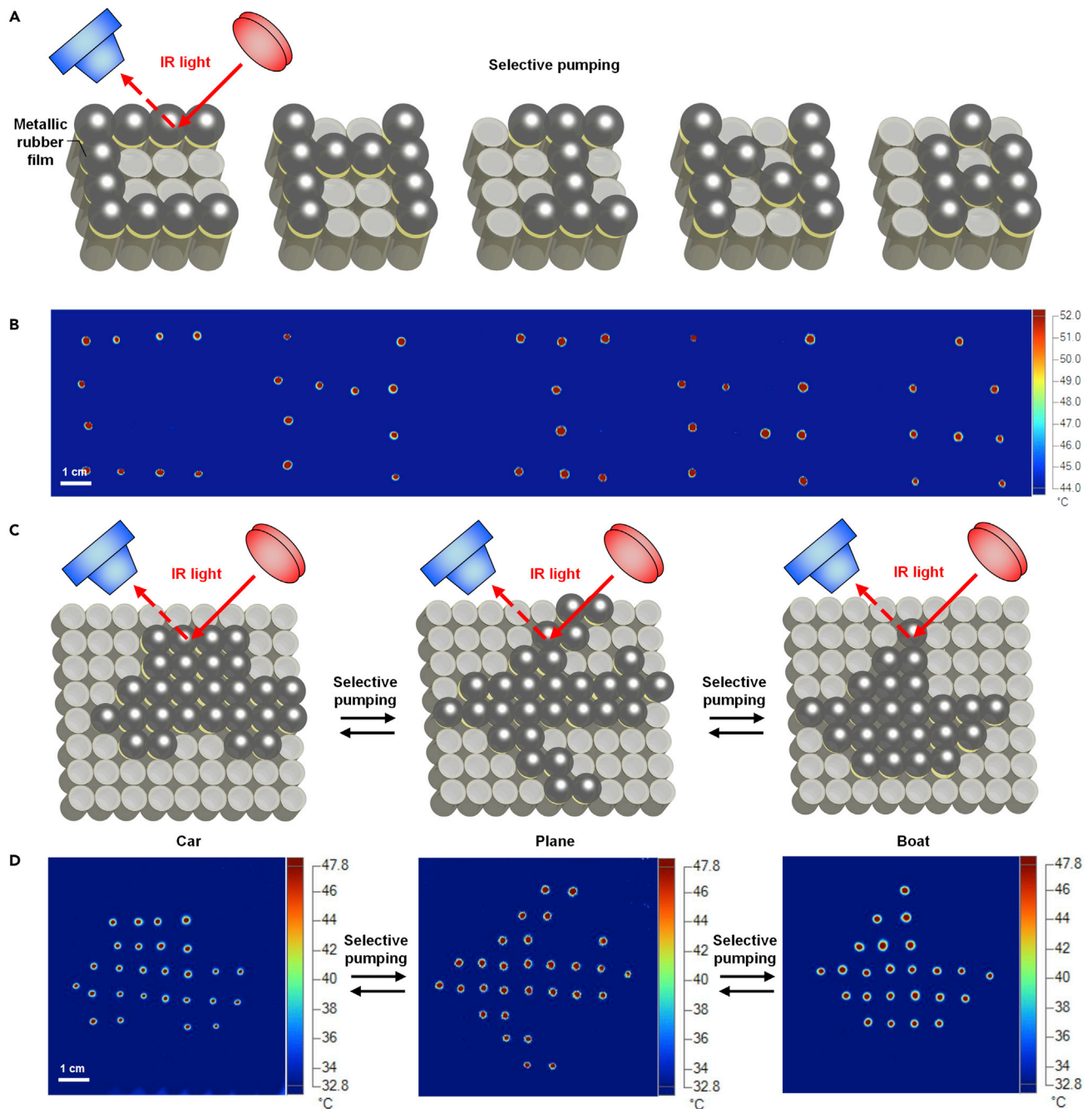
Figure 6. Changeable IR display and camouflage

(A) Schematic diagram of patterns of "C," "H," "I," "N," and "A" by selectively pumping certain tubes in 4 × 4 arrays to change their local IR reflection behaviors.

(B) IR images of displaying according "C," "H," "I," "N," and "A" patterns.

(C) Schematic diagram of changeable IR patterns, including a "car," a "plane," and a "boat," by selectively pumping certain tubes in 9 × 8 arrays.

(D) IR images of corresponding patterns. The changes in apparent temperature are represented by changes in color.

STAR★METHODS

Detailed methods are provided in the online version of this paper and include the following:

- KEY RESOURCES TABLE

- RESOURCE AVAILABILITY
  - Lead contact
  - Materials availability
  - Data and code availability
- METHOD DETAILS
  - Fabrication of the Janus rubber films
  - Fabrication of the adaptive IR reflection tube
  - Characterization

SUPPLEMENTAL INFORMATION

Supplemental information can be found online at https://doi.org/10.1016/j.isci.2021.102430.

AUTHORS CONTRIBUTION

B. S. and L.P. designed the experiments, analyzed the data, and wrote the manuscript. L.P., and J.H. carried out the experiments, discussed the results, and performed theoretical calculations. B.S., L.P., J.H., and R. Z. discussed and revised the manuscript.

DECLARATION OF INTERESTS

The authors declare no competing interests.

REFERENCES

Cai, L., Song, A.Y., Wu, P., Hsu, P.C., Peng, Y., Chen, J., Liu, C., Catrysse, P., Liu, Y., Yang, A., et al. (2017). Warming up human body by nanoporous metallized polyethylene textile. Nat. Commun. 8, 496.

Chandrasekhar, P., Zay, B.J., Mcqueeney, T.M., Scara, A., and Douglas, D. (2003). Conducting polymer (cp) infrared electrochromics in spacecraft thermal control and military applications. Synth. Met. 135, 23–24.

Chandrasekhar, P., Zay, B.J., Birur, G.C., Pierson, E.D., Kauder, L., and Swanson, T. (2002). Large, switchable electrochromism in the visible through far-infrared in conducting polymer devices. Adv. Funct. Mater. 12, 95–103.

Dai, L., Chen, S., Liu, J., Gao, Y., Zhou, J., Chen, Z., Cao, C., Luo, H., and Kanehira, M. (2013). F-doped VO₂ nanoparticles for thermochromic energy-saving foils with modified color and enhanced solar-heat shielding ability. Phys. Chem. Chem. Phys. 15, 11723–11729.

Granqvist, C.G., Arvizu, M.A., Pehlivan, B., Qu, H.Y., Wen, R.T., and Niklasson, G.A. (2017). Electrochromic materials and devices for energy efficiency and human comfort in buildings: a critical review. Electrochim. Acta 259, 1170–1182.

Gu, W., Tan, J.W., Chen, J., Zhang, Z., and Ji, G. (2020). Multifunctional bulk hybrid foam for

infrared stealth, thermal insulation, and microwave absorption. ACS Appl. Mat. Inter. 12, 28727–28737.

Golnaz, I., and Marco, L. (2018). Bioinspired stimuli-responsive color-changing systems. Adv. Mater. 30, 1707069.

Hu, Y., Zhong, H., Wang, Y., Lu, L., and Yang, H. (2018). TiO₂/antimony-doped tin oxide: highly water-dispersed nano composites with excellent IR insulation and super-hydrophilic property. Sol. Energy Mater. Sol. Cells 174, 499–508.

Hong, S., Shin, S., and Chen, R. (2020). An adaptive and wearable thermal camouflage device. Adv. Funct. Mater. 30, 1909788.

Jiang, S., Miao, D., Xu, J., Shang, S., Ning, X., and Zhu, P. (2016). Preparation and characterization of shielding textiles to prevent infrared penetration with Ag thin films. J. Mater. Sci. Mater. Electron. 28, 3542–3547.

Ji, H., Liu, D., Zhang, C., and Cheng, H. (2018). VO₂/ZnS core-shell nanoparticle for the adaptive infrared camouflage application with modified color and enhanced oxidation resistance. Sol. Energy Mater. Sol. Cells 176, 1–8.

Ke, Y., Zhou, C., Zhou, Y., Wang, S., Chan, S.H., and Long, Y. (2018). Emerging thermal-responsive materials and integrated techniques

targeting the energy-efficient smart window application. Adv. Funct. Mater. 28, 1800113.

Lee, S.J., Choi, D.S., Kang, S.H., Yang, W.S., Nahm, S., Han, S.H., and Kim, T. (2019). VO₂/WO₃–based hybrid smart windows with thermochromic and electrochromic properties. ACS Sustain. Chem. Eng. 7, 7111–7117.

Liu, M., Su, B., Kaneti, Y.V., Chen, Z., Tang, Y., Yuan, Y., Gao, Y., Jiang, L., Jiang, X.C., and Xu, A.B. (2016). Dual-phase transformation: spontaneous self-template surface-patterning strategy for ultra-transparent VO₂ solar modulating coatings. Acs Nano 11, 407–415.

Li, M.Y., Liu, D.Q., Cheng, H.F., Peng, L., and Zu, M. (2020a). Manipulating metals for adaptive thermal camouflage. Sci. Adv. 6, eaba3494.

Li, M.Y., Liu, D.Q., Cheng, H.F., Peng, L., and Zu, M. (2020b). Graphene-based reversible metal electrodeposition for dynamic infrared modulation. J. Mater. Chem. C 8, 8538–8545.

Leung, E.M., Escobar, M.C., Stiubianu, G.T., Jim, S.R., Vyatskikh, A.L., Feng, Z., Garmer, N., Patel, P., Naughton, K.L., Follador, M., et al. (2019). A dynamic thermoregulatory material inspired by squid skin. Nat. Commun. 10, 1947.

Morin, S.A., Shepherd, R.F., Kwok, S.W., Stokes, A.A., Nemiroski, A., and Whitesides, G.M. (2014).

Camouflage and display for soft machines. Science *337*, 828–831.

Mandal, J., Du, S., Dontigny, M., Zaghib, K., Yu, N., and Yang, Y. (2018). $Li_4Ti_5O_{12}$: a visible-to-infrared broadband electrochromic material for optical and thermal management. Adv. Funct. Mater. *28*, 1802180.

Mathger, L.M., Denton, E.J., Marshall, N.J., and Hanlon, R.T. (2009). Mechanisms and behavioural functions of structural coloration in cephalopods. J. R. Soc. Interf. *6*, 149–163.

Mathger, L.M., and Hanlon, R.T. (2007). Malleable skin coloration in cephalopods: selective reflectance, transmission and absorbance of light by chromatophores and iridophores. Cell Tissue Res *329*, 179–186.

Peng, L., Fan, W., Li, D., Wang, S., Liu, Z., Yu, A., and Jiang, X. (2020). Smart thermal management textiles with anisotropic and thermoresponsive electrical conductivity. Adv. Mater. Tech. *5*, 201900599.

Phan, L., Kautz, R., Leung, E.M., Naughton, K.L., Van Dyke, Y., and Gorodetsky, A.A. (2016). Dynamic materials inspired by cephalopods. Chem. Mater. *28*, 6804–6816.

Salihoglu, O., Uzlu, H.B., Yakar, O., Aas, S., Balci, O., Kakevov, N., Balci, S., Olcum, S., Süzer, S., and Kocabas, C. (2018). Graphene based adaptive thermal camouflage. Nano Lett. *18*, 4541–4548.

Tian, Y., Zhang, X., Dou, S., Zhang, L., Zhang, H., Lv, H., Wang, L., Zhao, J., and Li, Y. (2017). A comprehensive study of electrochromic device with variable infrared emissivity based on polyaniline conducting polymer. Sol. Energy Mater. Sol. Cells *170*, 120–126.

Wang, Q., Gossweiler, G.R., Craig, S.L., and Zhao, X. (2014). Cephalopod-inspired design of electro-mechano-chemically responsive elastomers for on-demand fluorescent patterning. Nat. Commun. *5*, 4899.

Xu, F., Cao, X., Luo, H., and Jin, P. (2018a). Recent advances in VO_2-based thermochromic composites for smart windows. J. Mater. Chem. C *6*, 1903–1919.

Xu, C., Stiubianu, G.T., and Gorodetsky, A.A. (2018b). Adaptive infrared-reflecting systems inspired by cephalopods. Sci *359*, 1495–1500.

Xu, C., Escobar, M.C., and Gorodetsky, A.A. (2020). Stretchable cephalopod-inspired multimodal camouflage systems. Adv. Mater. *32*, 1905717.

Yu, C., Li, Y., Zhang, X., Huang, X., and Rogers, J.A. (2014). Adaptive optoelectronic camouflage systems with designs inspired by cephalopod skins. Proc. Natl. Acad. Sci. U S A *111*, 12998–13003.

Yang, J., Zhang, X., Zhang, X., Wang, L., Feng, W., and Li, Q. (2021). Beyond the visible: bioinspired infrared adaptive materials. Adv. Mater. *33*, 2004754.

Zhu, H., Li, Q., Zheng, C., Hong, Y., and Qiu, M. (2020). High-temperature infrared camouflage with efficient thermal management. Light Sci. Appl. *9*, 60.

STAR★METHODS

KEY RESOURCES TABLE

REAGENT or RESOURCE	SOURCE	IDENTIFIER
Chemicals, peptides, and recombinant proteins		
Commercial rubber dispersion (polyisoprene, 50 wt%)	Suzhou innovation latex Co., Ltd.	NA
Aluminum coated mica microsheets (AMSs)	Ruicai Technology Co. Ltd.	NA
Calcium nitrate tetrahydrate ($Ca(NO_3)_2 \cdot 4H_2O$)	Shanghai Aladdin Bio-Chem Technology Co., Ltd.	CAS#13477-34-4
Porcellanite	Guangzhou Yifeng Chemical Co., Ltd.	NA
Software and algorithms		
COMSOL Multiphysics	COMSOL	http://cn.comsol.com/

RESOURCE AVAILABILITY

Lead contact

Further information and requests for resources and reagents should be directed to and will be fulfilled by the lead contact, Bin Su (subin@hust.edu.cn).

Materials availability

This study did not generate new unique reagents.

Data and code availability

This study did not generate/analyze.

METHOD DETAILS

Fabrication of the Janus rubber films

The Janus rubber films were prepared by two steps: first, a metallic plate coated with a thin layer of pre-treated water dispersion (1 g calcium nitrate and 1.5 g porcellanite in 20 g water) was first submerged in the raw rubber dispersion (with a weight-average molecular weight of ~160,000), yielding a thin rubber film. AMSs were mixed with rubber dispersion under stirring (the weight ratio of AMSs to the raw rubber dispersion was 1/5). Then, the plate was submerged into an AMSs/rubber composite dispersion. Finally, the plate was heated at 80°C for 3 h, yielding the Janus rubber films with the evaporation of organic solvent.

Fabrication of the adaptive IR reflection tube

The IR reflecting tube was composed of a steel or plastic tube (length: 15 cm, inner diameter: 1 cm), a 1.5 × 1.5 cm^2 Janus rubber film, a hollow steel/plastic plate with a hole diameter of 1.1 cm, and a sealing O-ring. The tube was covered and sealed by the Janus rubber film on the top (the AMSs/rubber layer stayed upwards). The bottom of the tube was sealed and connected with a propulsion setup to provide controlled pumping forces. Gas and liquid pressure or mechanical forces could both provide desired pumping forces. In this study, pneumatic pumping was chosen as a representative pumping strategy (pumping pressure was around 50 kPa). For the display by assembled tube arrays, plastic IR reflecting tubes with 0.4 cm in diameter and 1 cm in length (mainly consideration is its light weight) were used. The tubes were arranged into up to 9 × 8 arrays. Each tube can be manually or computer controlled to pump or remain separately.

Characterization

SEM images of the Janus rubber films were obtained by the field emission scanning electron microscope (FEI Nova 450, America). The transmittance and reflection spectra were measured using Solid Spec-3700 UV-visible near-infrared spectrophotometer (Shimadzu, Japan). Five points were measured, and the average valued were calculated. Data were represented as mean $\pm$ sem (n = 5). Mechanical strength

of the rubber film was conducted by a tensile tester (HZ-1007C, Dongguan Lixian Instrument Technology Co., Ltd, China). Microscopy images and surface roughness of the Janus rubber film were observed by a microscope (DSX 510, OLYMPUS). IR diffuse reflection was measured by PerkinElmer Spectrum 100 spectrophotometer. The thickness of the Janus rubber film was measured by using a digital caliper (five points were measured, and the average valued were calculated). The digital images were all recorded by a digital camera (Canon EOS 800D). Infrared images were taken by the infrared camera (Fluke Ti401 PRO, USA). The IR source was an IR radiation heater (1200 W) and kept 1.5 meters away from the samples. The weight average molecular of the rubber dispersion was characterized by Waters GPC1525.

Electromagnetic (EM) wave simulations were conducted using commercial finite element method (FEM) software (COMSOL Multiphysics). The optical constants (n, k) of aluminum were taken in from 1000 nm. The boundary conditions of the simulation region were set to PML (perfectly matched layer) at the z direction and periodic at the x and y directions. The plane wave model was used as an incident beam source and traveled along the y axis. The numerical models are constructed based on experimental data, and all models have a constant mass or volume. The thickness of the top Janus rubber film in simulation study was adjusted from 25 to 10 μm before and after stretching with 100% strain, respectively.